



Sunshine and solar power in the UK

Greg Spellman¹ · Danielle Bird¹

Received: 9 May 2023 / Accepted: 16 October 2023 / Published online: 22 November 2023
© The Author(s) 2023

Abstract

Solar power is an increasingly important source of clean energy even for a relatively cloudy mid-latitude nation such as the UK. Using areal sunshine series published by the UK Met Office, this study describes the continuing brightening trend that has also been observed since the mid-1980s around the world. The use of the automated Lamb weather type system is explored, particularly the surface synoptic indices developed by Jenkinson and Collison. There is a strong association between sunshine duration (via cloudiness) and circulation features such as anticyclonicity; however, there is no surface-level circulation trend observed that can explain the brightening.

1 Introduction

Solar radiation is the ultimate energy source for the Earth-atmosphere system, ensuring that the planet is thermally optimal for the evolution of life, driving the hydrological cycle and enabling photosynthesis; yet, the sun has an important societal value as a clean energy source. In the UK, harnessing increasing amounts of solar energy is critical to both maintaining a secure energy supply and the transition to net zero carbon. The UK is not a sunny country; however, as a consequence of the long daylight duration in the summer months, large amounts of solar energy are attainable. In 2014, Burnett et al. commented that solar energy generation in the UK was increasing rapidly, providing both heat energy and generation of electricity. This trend has continued, due to more cost-effective solar technologies, to the point that solar power generated 12.47 Twh of electricity in 2021, three times the total of 2014 (Ritchie and Roser 2022). This represented around 4% of all electricity generation in the UK, the third largest form of renewables after wind and biomass and, according to BP (2022), the country has the fifth largest installed solar power capacity in Europe (13.69 GW) and the twelfth largest globally (Table 1). In addition to the enhanced energy potential, greater sunshine, particularly in higher latitudes, has positive societal benefits such as the promotion of exercise, well-being and improved mental

health (Taniguchi et al. 2022), a boost for domestic tourism (Taylor and Ortiz 2001), and even the enhanced productivity of some agriculture (Arnell and Freeman 2021).

The solar radiation resource varies spatially with latitude, altitude and regional climatic factors that control the amount of cloudiness and, hence, the transparency of the atmosphere. Temporal variations are a consequence of fundamental astronomical factors such as the hours of daylight and solar altitude; however, research in the last two decades has suggested a strong directional trend in incident radiation at many locations. Wild (2009) presents evidence of a global brightening trend which has increased the amount of surface solar radiation receipt since the mid-1980s. Instruments that measure solar radiation have been available for many years, and a small number of lengthy historic datasets exist for Europe and North America (GEBA 2022); however, global coverage is sparse. Fortunately, a good proxy is sunshine duration (SD) which is strongly correlated to solar radiation and has been routinely measured at many weather stations.

This study uses gridded SD data based on observational data provided by the UK Meteorological Office (UKMO) for the period 1919–2021. We aim to explore the variability in SD in the series for England and to identify if any continuing directional trends can be identified. Using a well-known synoptic weather typing technique, we investigate the role of surface atmospheric circulation patterns on SD via changes in, principally, cloudiness over the England and its regions.

✉ Greg Spellman
Greg.spellman@northampton.ac.uk

¹ Faculty of Arts, Science and Technology, University of Northampton, Northampton NN1 5PH, UK

Table 1 Solar power generating capacity by country in GW (BP 2022)

Rank	Country	Solar capacity (GW 2021)	Rank	Country	Solar capacity (GW 2021)
1	China	306.40	9	Vietnam	16.66
2	USA	93.71	10	France	14.71
3	Japan	74.19	11	The Netherlands	14.25
4	Germany	58.46	12	UK	13.69
5	India	49.34	13	Spain	13.65
6	Italy	22.69	14	Brazil	13.05
7	Australia	19.07	15	Ukraine	8.06
8	South Korea	18.16	16	Turkey	7.82

2 Measurement of solar radiation and sunshine

Quantifying the solar resource, both spatially and temporally, is important for planning solar power generation. In addition, projected climate change scenarios by changing atmospheric conditions will affect the supply of this energy (Burnett et al. 2014). The important energy fluxes are global irradiance (total downwelling solar radiation) and its component parts—direct radiation from the sun and diffuse radiation that comes from other parts of the sky. In the UK, radiation is measured daily (and, sometimes, hourly) at several locations. There are long, but incomplete, records at a small number of currently operating stations, such as Lerwick, Scotland (1952), Aberporth, Wales (1957), Sutton Bonington, Midlands (1963) and East Malling, South East (1963) (*start dates in parentheses*).

Nevertheless, in the absence of long-term reliable solar radiation data, empirical relationships originally developed by Prescott (1940), and later updated by Suehrck (2000), can be used to estimate solar radiation from observed hours of sunshine; SD is a more widespread measure than solar radiation and is routinely collected at climate stations around the world. Related cloud cover data (*i.e.* cloudiness) are based on subjective visual estimates and are less useful than SD. Sunshine duration was historically measured using Campbell-Stokes (C-S) sunshine recorders which consist of a solid glass ball positioned above a semi-circular sun card. As bright sunshine passes through the ball, the beam is concentrated so as to result in a burn into the sun card. The length of the burnt trace is then converted into hours of sunshine.¹

For the past two decades the UKMO has been progressively replacing C-S recorders with automatic sensors

produced by the manufacturer Kipp & Zonen. Deficiencies of the C-S recorders include the fact that sun cards need to be extracted, examined and then manually replaced every day that the energy levels required to burn a trace on the card vary with environmental conditions, and even that dew or frost on the surface of the sphere can reduce the intensity of sunlight passing through. Automatic sensors are, therefore, more cost effective and, arguably, more accurate. On the other hand, the homogeneity of long-term records of sunshine is reduced if there is a low correlation between C-S recordings and automated sensors. Matuszko (2015) suggests that this could prompt the wrong conclusion about the long-term variability of sunshine. There have been some investigations using overlapping measurements (*e.g.* Matuszko 2015; Urban and Zajac 2017) for a small number of locations with long enough simultaneous records, and given the higher sensitivity of automatic sensors, it could be expected that they would yield larger SD totals than those recorded by traditional instruments.

The threshold for ‘sunshine/no sunshine’ is defined by the World Meteorological Organization (WMO 2008) as the ‘the duration of the period for which the direct solar irradiance exceeds 120 W/m²’; yet, for the C-S recorder, the threshold necessary to produce a burn averages 170 Wm⁻², with a range from 106 to 285 Wm⁻² (Painter 1981). Furthermore, C-S instruments do not perform well when the sun is low (3–5°) over the horizon, for instance, in the winter months or at each end of the day (Matuszko 2012). The majority of comparative studies undertaken suggest that there is a complex pattern of disagreement with both positive and negative differences between instruments, and, generally, systematic bias has been identified (*e.g.* Matuszko 2012; Urban and Zajac 2017). Largest differences (of both positive and negative directions) occur when there are clouds of different layers or scattered clouds. Srinivasa et al. (2019) found, on average, that Kipp & Zonen sunshine durations were higher than Campbell-Stokes sunshine durations at four sites in New Zealand, with the difference ranging from 2% at Invercargill to 17% at Hokitika. Differences on individual days were smaller on ‘mostly sunny’ or ‘cloudy days’ and higher on days with periodic cloud cover. Efforts by Kerr and Tabony (2004) and Legg (2014) in the UK have explored the extent to which the C-S observations and sensor measurements differ and develop a quadratic model to adjust measurements from Kipp & Zonen sensors so that errors in estimates of ‘C–S equivalent’ monthly sunshine totals for individual stations have been reduced to less than 3% on average.

Sunshine duration measurements have long been shown to be comparable with measurements of solar irradiance and have been useful in the analysis of this resource. For instance, Fig. 1 shows the strong correlation between total monthly solar insolation (Kilojoules m⁻²) and monthly

¹ For further details the C-S recorders produced by Lambrecht can be viewed here https://novalynx.com/manuals/16030_16040_Manual.pdf

Fig. 1 Relationship between total monthly insolation (KJm^2) and sunshine duration (hours) at two sites in the UK—Camborne in SW England (1982–2020) and Sutton Bonington (1970–1999) in the Midlands region

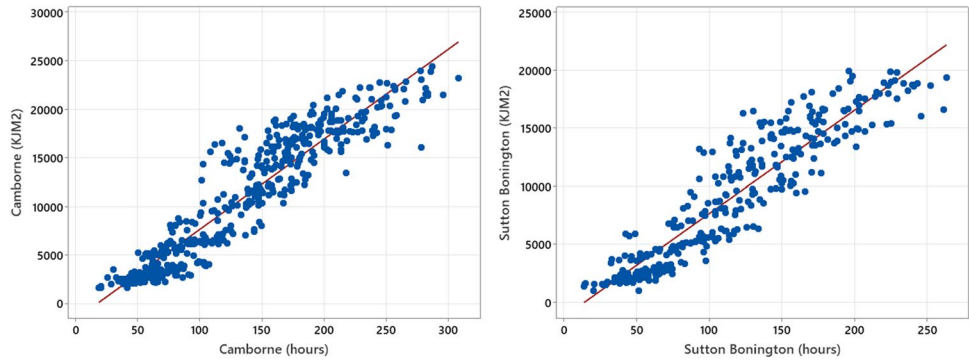
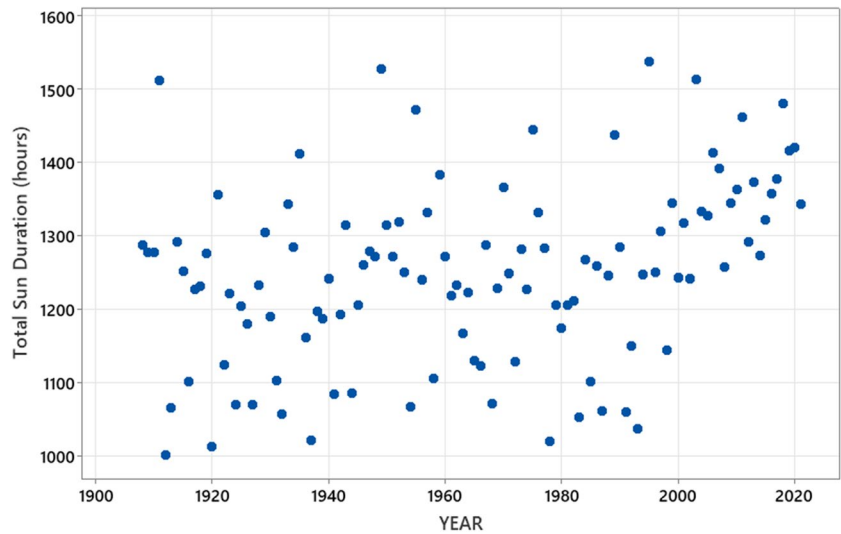


Fig. 2 Annual sunshine duration (hours) observed at Bradford, UK (1908–2021). Note from August 2003 sunshine data taken from an automatic Kipp & Zonen sensor. Annual mean = 1249.7 h (SD 123.1)



sunshine duration (hours) at Camborne in the southwest of England ($R^2 = 87.3\%$, $F = 3200$; $p < 0.001$) and Sutton Bonington in the Midlands ($R^2 = 86.3\%$, $F = 2067$; $p < 0.001$). In Fig. 1, separate linear associations can be seen at low radiation levels. These represent observations in the winter months when the low altitude sun leads to low radiation receipt even when sunshine duration is relatively lengthy.

There are some very long records of monthly sunshine data in the UK. For instance, a 114-year monthly record exists for Bradford in the north of England from 1908 to current (Fig. 2). There is considerable year-to-year variability in the annual total (mean = 1250 h with a range of 536 h). For instance, one of the sunniest years on record, 1911 (1510 h), was followed by the dulllest year in 1912 (1001 h). Sunshine duration at any location is a function of time of year and day, and, therefore, a theoretical potential maximum amount can be calculated from the difference between the times of sunrise and sunset for each day and then totals for each month summed. In Bradford (in common with all locations in the British Isles), the mean monthly sunshine fraction (0.31) is relatively low compared to the global terrestrial mean and is obviously not constant (Fig. 3). The

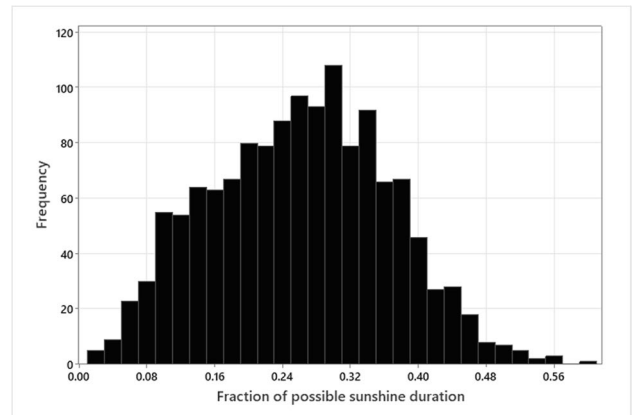


Fig. 3 Frequency distribution of mean monthly sunshine fraction (observed SD hours/maximum potential SD hours) for Bradford, UK (1908–2021)

sunshine fraction (observed SD hours/maximum potential SD hours) at any location is a response to the transparency of the atmosphere—a function of, primarily, cloudiness, atmospheric turbidity (amount of natural, such as large

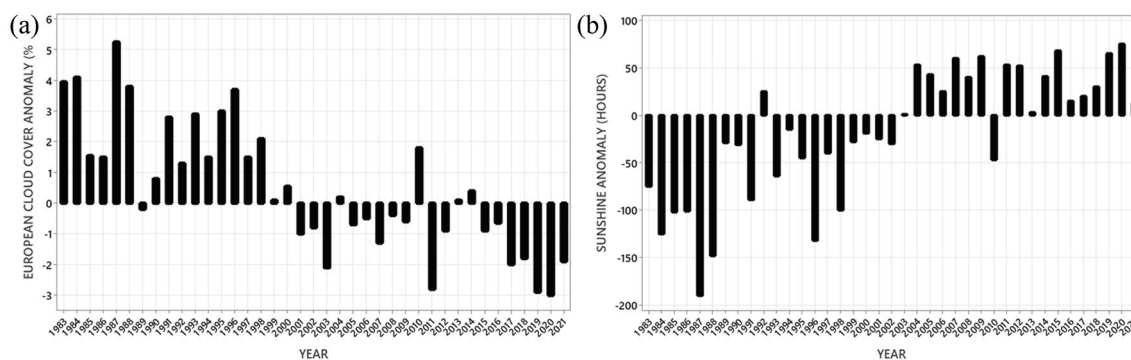


Fig. 4 **a** European cloud cover anomaly and **b** sunshine duration anomaly (from Copernicus 2022)

scale/nearby volcanic eruptions or anthropogenic aerosols) and solar altitude.

The ‘cloudiness’ of a location at any one time depends on a number of factors—presence or absence of cloud, cloud type, cloud thickness (or depth), cloud base height, micro-structure and water content per unit of volume, the distribution of clouds with respect to the position of the Sun’s disk in the sky and aerosol content of the atmosphere (Voigt et al. 2020). The increasing presence of aerosols in the atmosphere reduces the intensity of solar radiation by absorption and scattering; however, Sanchez-Romero et al. (2014) point out that small changes in direct solar radiation above the burning threshold are hard to detect, and, therefore, the impact of aerosols on SD is likely to occur just after sunrise and before sunset because of the long distance that the direct beam must travel to reach the Earth’s surface.

With respect to the changing nature of solar radiation, several studies, mostly based on the Global Energy Balance Archive (GEBA), have identified a widespread reduction in solar radiation received by the Earth from the 1950s to the 1980s, a phenomenon that has been called ‘*global dimming*’ (e.g. Stanhill and Cohen 2001; Liepert 2002). This was followed in the mid-1980s by stabilisation and recovery in many regions of the world termed ‘*global brightening*’ (Wild et al. 2005; Wild 2009; Wang et al. 2012; Augustine and Dutton 2013). Reasons for the shifts in these trends have not been fully determined (Urban et al. 2018); however, changes in the transparency of the atmosphere due to variations in anthropogenic aerosol emissions and/or cloudiness are clearly the major factors.

The most important meteorological determinant of the fraction of solar radiation reaching the Earth’s surface is cloud cover, but attribution of dimming to aerosol change suggests anthropogenic rather than natural origins, and this view was supported by the IPCC (2007) who reported work by Alpert et al. (2005), indicating that reductions in radiation were largely confined to urban areas near sources of pollution. Streets et al. (2009) suggested that the increase in incident radiation was due to the improvement in atmospheric

management from the early eighties onwards. Cutforth and Judiesch (2007) and Stanhill et al. (2014) have suggested that changes in cloud cover rather than aerosol load were the major cause of solar dimming and brightening during the last half century.

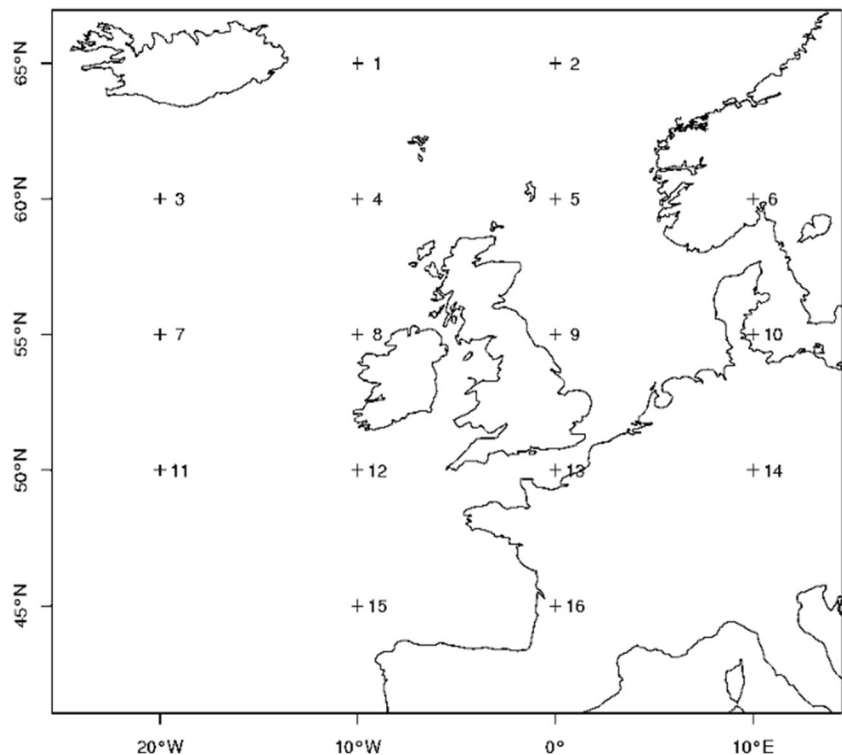
Time series of ground-based SD observations mirror patterns in the radiation series. Sanchez-Lorenzo et al. (2008), for example, used 72 sunshine duration records on the Iberian Peninsula and detected a decrease from the 1950s to the early 1980s, followed by a positive trend up to the end of the twentieth century matching the ‘dimming’ and the subsequent ‘brightening’ in the solar radiation data. Since the early 1980s, satellite observations have been able to obtain spatially-complete estimates of clouds and surface radiation and also of sunshine duration (Copernicus 2022). These have identified a general trend towards less cloud cover over Europe during the last four decades (Fig. 4a) and a consequent trend towards increased sunshine duration (Fig. 4b).

3 Data sources and method

3.1 Sunshine duration data

Sunshine duration is one of the meteorological variables included in the UKMO climate series (1919–2022) which are derived from the *HadUK-Grid* dataset. This is a set of station-based observations (*i.e.* temperature, rainfall, sunshine) from the UKMO’s Integrated Data Archive System (MIDAS) that are interpolated onto a regular $1\text{ km} \times 1\text{ km}$ grid (Hollis et al. 2019). The sunshine series includes 290 stations on average, and the estimation procedure combines multiple regression with inverse-distance weighted interpolation. Geographic and topographic factors, such as easting and northing, elevation and relief and urban and coastal effects are taken into account either through normalisation with regard to the 1981–2010 average climate, or as independent variables in regression models (Hollis et al. 2019). Local variations are incorporated through the

Fig. 5 Location of grid points used in Jenkinson and Collison method



spatial interpolation of residuals. Grid values are then averaged over areas including the whole of the UK, England, Wales, Scotland, Northern Ireland and UK climate districts (for instance, in England—Southwest, South East, East Anglia, Midlands, North West and North East). The majority of the stations recording SD in the UKMO network use a Campbell-Stokes (C-S) recorder. However, a significant proportion of the stations now use a Kipp & Zonen CMP3 pyranometer (first installed in 2000). The two instruments are not identical, and, therefore, monthly totals from automatic sensors are adjusted to ‘C-S equivalent’ values using a methodology described by Kerr and Tabony (2004) and Perry (2007). The main focus of this current study has been on patterns in sunshine duration, but some daily insolation data were also sourced from MIDAS.

3.2 Synoptic classification technique

Daily atmospheric circulation patterns for the British Isles are described by the Lamb weather type classification (Lamb 1972). This study employs the automated version developed by Jenkinson and Collison (JC) (1977). This is a well-used technique for classifying atmospheric circulation and has been applied to many locations such as Scandinavia (Linderson 2001), Serbia (Putnikovic et al. 2016), the Iberian Peninsula (Miró Cubells et al. 2020), Siberia (Osipova and Osipov 2022), Chile (Sarricolea et al. 2018) and China

(Wang and Sun 2019). The classification is commonly used to analyse environmental phenomena including temperature (e.g. Chen 2000), rainfall (e.g. Spellman 2017) and a range of circulation-related phenomena such as air pollution (e.g. Pope et al. 2016) and human mortality (Psistaki et al. 2020). The Jenkinson-Collison technique uses sea-level pressure data recorded at 12 UTC obtained from NCEP reanalysis (Kalnay et al. 1996) for a 16-point grid centred over the British Isles (Fig. 5). It determines seven indices of circulation which describe flow direction, strength and the degree of quasi-geostrophic vorticity (curvature of sea level isobars) which are used to classify each day into one of 27 weather types using the formula and rules below,

P is the mean sea-level pressure (hPa) across the grid.

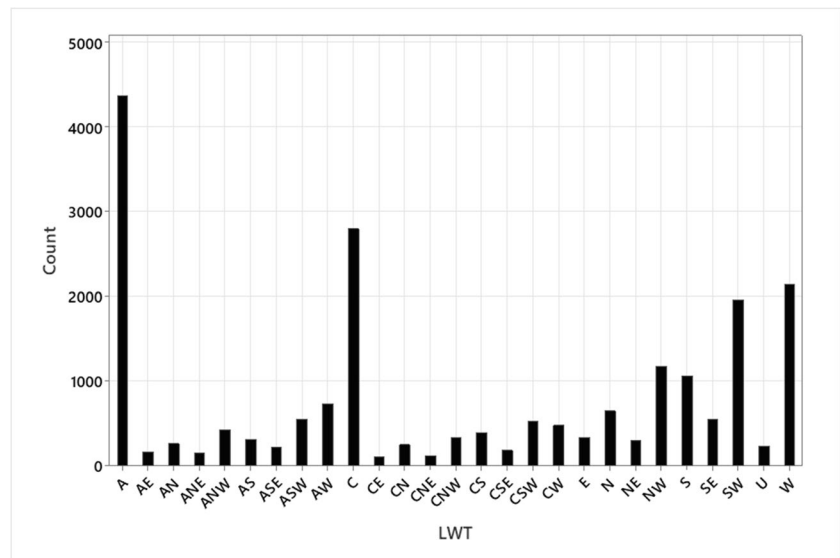
$$P = \sum_{i=1}^{16} P_i / 16 \quad (1)$$

The components of the geostrophic wind are W , the westerly (zonal) component calculated as the pressure gradient between 45° N and 65° N, and S , the southerly (meridional) component, calculated as the pressure gradient between 20° W and 10° E,

$$W = 0.5(p_{12} + p_{13}) - 0.5(p_4 + p_5) \quad (2)$$

$$S = 1.74 [0.25(p_5 + 2p_9 + p_{13}) - 0.25(p_4 + 2p_8 + p_{12})] \quad (3)$$

Fig. 6 Lamb weather type frequency (Jenkinson and Collison automated types) 1948–2021



F is the combined wind speed of W and S and is calculated by,

$$F = \sqrt{W^2 + S^2} \tag{4}$$

Shear vorticity (westerly (ZW) and southerly (ZS) shear vorticity) is calculated for the centre (55° N, 5° E),

$$ZW = 1.07[0.5(p_{15} + p_{16}) - 0.5(p_8 + p_9) - 0.95[0.5(p_8 + p_9) - 0.5(p_1 + p_2)]] \tag{5}$$

$$ZS = 1.52[0.25(p_6 + 2p_{10} + p_{14}) - 0.25(p_5 + 2p_9 + p_{13}) - 0.25(p_4 + 2p_8 + p_{12}) + 0.25(p_3 + 2p_7 + p_{11})] \tag{6}$$

$$Z = ZW + ZS \text{ is the total shear vorticity} \tag{7}$$

All the indices have units of hPa/(10° latitude) at 55° N and are geostrophic. The various constants appearing in the equations are derived from the fact that the grid cells represent areas of different sizes. The coefficient in Eq. 3, 1.74, is $\frac{1}{\cos\theta}$; in Eq. 4, 1.07 and 0.95 are $\frac{\sin\theta}{\sin(\theta-5^\circ)}$ and $-\frac{\sin\theta}{\sin(\theta+5^\circ)}$, respectively; and in Eq. 5, 1.52 is $\frac{1}{2}(\cos(\theta)^2)$.

Daily weather types are then determined using the following five rules:

- (1) The direction of flow is $\tan^{-1}(W/S)$. Direction is determined as follows: if W is negative and S is positive, add 180° ; if W is positive and S is negative, add 360° ; if W is negative and S is positive, add 180° ; if both W and S are negative, add 0° . These angles are then converted into eight compass

points (NE, E, SE, S, SW, W, NW, N) where NE = $22.5^\circ - 67.49^\circ$ and so on.

- (2) If $|Z| < F$, then flow is straight and the weather type is pure directional (e.g. E) according to rule (1).
- (3) If $|Z| > 2F$, then the pattern is strongly cyclonic if $|Z| > 0$ or anticyclonic if $|Z| < 0$ (e.g. A).
- (4) If Z lies between F and $2F$, the flow is hybrid (e.g. CNE). It is a cyclonic hybrid if $|Z| > 0$ or anticyclonic if $|Z| < 0$. Direction is determined using rule (1).
- (5) If F and $|Z|$ are both less than 6, an undetermined (U) weather type is reported.

The catalogue is therefore composed of three main groups of weather types and one undetermined type (U). There are eight pure directional types—NE, E, SE, SW, W, NW and N, two types based wholly on geostrophic vorticity—C (cyclonic) and A (anticyclonic) and then sixteen hybrid types (CNE, CE, CSE, CS, CSW, CW, CNW, CN, ANE, AE, ASE, AS, ASW, AW, ANW and AN).

The outcome is a 37–621-day catalogue for the period 1919–2021 (Fig. 6). Some limitations of the system have been noted. The method fits a classification system for daily 12UTC pressure patterns; however, these are likely to change within a 24-h period and also vary spatially across the classified window. Furthermore, moving from continuous information to discrete categories entails a certain amount of lost information as there will inevitably be variability within classes. Nominal data does not capture the intensity of circulation as, for example, all storms centred in the classification window are termed ‘C’ irrespective of their severity and possibly very different meteorology (see Fig. 7a–d). To some extent, this can be

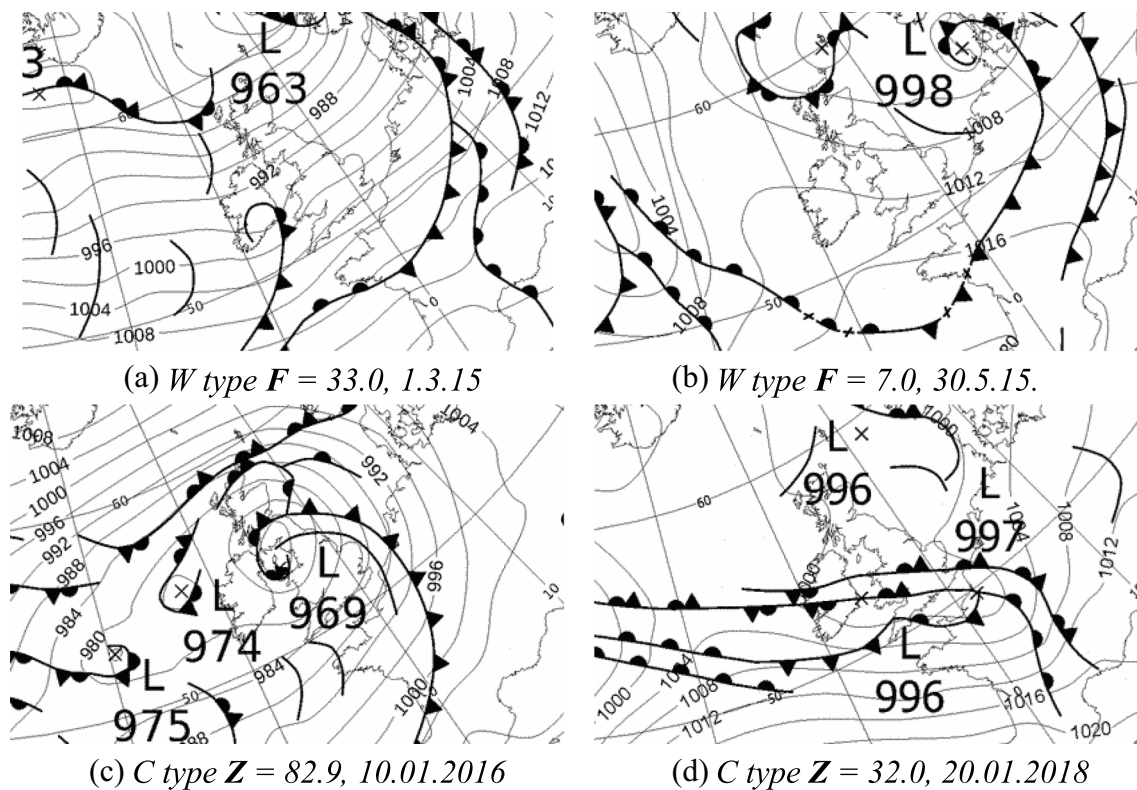


Fig. 7 a–d Variation of weather type ‘intensity’

circumvented by employing the individual indices in any synoptic analysis. For instance, the degree of cyclonicity can be explored using Z values alone. All things being equal a cyclonic day with a high negative Z value will be considerably more unstable than one with a comparatively low value. Likewise, consideration of the magnitude of the westerly and southerly components is especially useful in a location like the British Isles, where the nature of the atmosphere (and potentially cloud-forming mechanisms) are strongly related to wind direction. In this study, we use monthly mean index values to examine the variability in the monthly series. Daily weather types are also used to examine daily solar radiation amounts at selected stations.

Further criticism of the system can be directed towards the absence of information about fronts. Fronts are transition zones between two air masses which often have contrasting properties. Meteorology is varied depending on the type of front (warm, cold, occluded) and its level of activity, but differences between two air masses often produce considerable cloud coverage which will have an impact on measured SD. The examples in Fig. 8 a and b show 2 days which are both classified as *W* but with differing frontal activity and cloudiness.

The starting point of any synoptic analysis is a mechanism that relates the climatic variable being studied to circulation. Atmospheric dynamics will determine the temperature

structure, moisture advection, turbulence, depth of instability and other factors that influence cloudiness (Voigt et al. 2020). In the case of the British Isles, this could be at a large scale and be controlled by the position of the polar jet stream and subsequent tracks of mid-latitude storms. Alternatively, anticyclonic systems strengthen descent of air, enhancing lower-tropospheric stability which could either suppress cloud development or promote low-level clouds (Grise and Polvani 2014). The North Atlantic Oscillation (NAO) is the dominant mode of large-scale variability over the North Atlantic region and this will have a major control on cloud over the British Isles (Pozo-Vázquez et al. 2004). Using satellite imagery, Papavasileiou et al. (2020) showed that positive phases of the NAO are associated with more high-level clouds along the storm track (55° N) and the subpolar Atlantic and less high-level clouds poleward and equatorward of it.

The JC technique captures finer detail both spatially and temporally of circulation variability than the NAO. Directional types over the British Isles introduce distinct air masses (with respect to near surface temperature, humidity, lapse rates and stability conditions), and atmospheric conditions are then modified by anticyclonic or cyclonic curvature of air flow. Typical weather characteristics accompanying each weather type will vary with season and these are noted in Table 2.

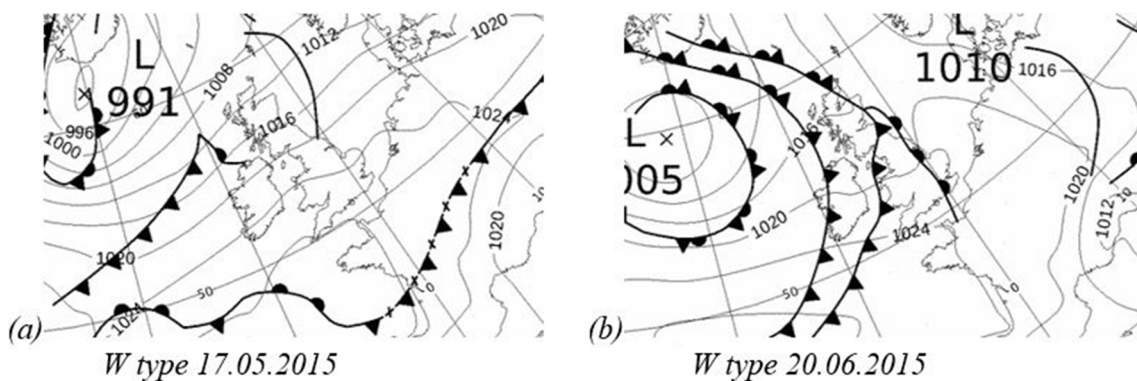


Fig. 8 Weather type classified with differing frontal activity and cloudiness

Table 2 Typical meteorological conditions in the British Isles accompanying more common weather types

General weather type	Weather characteristics
Anticyclonic	Subsiding air. Mainly dry with light winds. Some summer thunderstorms. Warm in summer and cold or very cold in winter. Generally clear skies, however, a significant feature of high pressure in winter (and sometimes in other seasons) is ‘anticyclonic gloom’ caused by extensive sheets of stratiform cloud when maritime air gets entrained in the circulation of high pressure and trapped under the subsidence inversion
Cyclonic	Ascending air. Depressions stagnating or passing over UK. Wet or disturbed weather with extensive cloudiness but also periods of sunshine
Westerly	Unsettled or changeable weather—most rain in N and W of UK. Mild and stormy in winter. Cool and cloudy in summer
North westerly	Cool with unstable changeable conditions—particularly in NW. There is often a diurnal cycle of cloudiness with clear mornings and evenings
Northerly	Cold weather in all seasons. Snow and sleet showers in winter—particularly in N and E. Unstable but often with low moisture content and, hence, clear skies in the south of the country
Easterly	Cold in autumn, winter and spring. Occasionally severe weather in south, with snow. This can be clear; however, stratiform cloud can drift in from the east particularly in winter
Southerly	Warm and thundery in spring and summer. Mild or cold in winter depending on airmass origin
South westerly	Very high rainfall totals over whole country. Warm moist airmass often with extensive cloud in winter

4 Results

4.1 Sunshine duration in England

The annual mean total of sunshine duration in the England series (1919–2021) is 1464 h (standard deviation = 116.9 h) with, on average, the sunniest month being June (191.5 h) when days are longest and the least sunshine occurs in December (45 h). Strikingly in Fig. 9, mean sunshine fractions are also lower in the winter half of the year. This is because the low altitude sun ensures that potential hours are even less likely to be approached by actual SD. Radiation passing through a sky with only scattered clouds has a stronger likelihood of being intercepted by cloud if the angle of incidence is low (or, in other words, at the extreme over the equator the overhead sun is only affected by those clouds directly underneath). Even in the south of England, the sun never does not

reach more than 15° above the horizon in mid-December compared to 62° at the summer solstice. The highest mean fraction is in May (0.39), despite the fact that greatest potential sunshine (over 500 h) is available in June and July, indicating that these latter months regularly experience more cloudiness. There is a higher frequency of northerly and easterly winds that occur in the spring compared to the other seasons of the year, and secondly, the summer monsoon effect (this is a far more subtle effect than the Asian monsoon) marks the return of the westerlies and typically occurs in mid-June. In May 2020, the mean sunshine fraction reached 0.62 (299.4 h, $z=2.94$) which accompanied unusually clear skies over much of NW Europe (Van Heerwaarden et al. 2021).

Sunshine duration for the England areal series is shown in Fig. 10 with the 3-year moving average. Although there is no discernible dimming trend in this dataset, there is a clear and significant ($F=7.30$, $p<0.05$, $R^2=17.3\%$) increase in sunshine from the mid-1980s. Since 2000, there is reduced

Fig. 9 Mean monthly sunshine fraction (observed SD hours/maximum potential SD hours) for England series 1919–2021. (For a central point in England 53° N, 1° W from the Astronomical Applications Department of the US Navy. https://aa.usno.navy.mil/data/Dur_OneYear. It is accepted there will be variation within this area.)

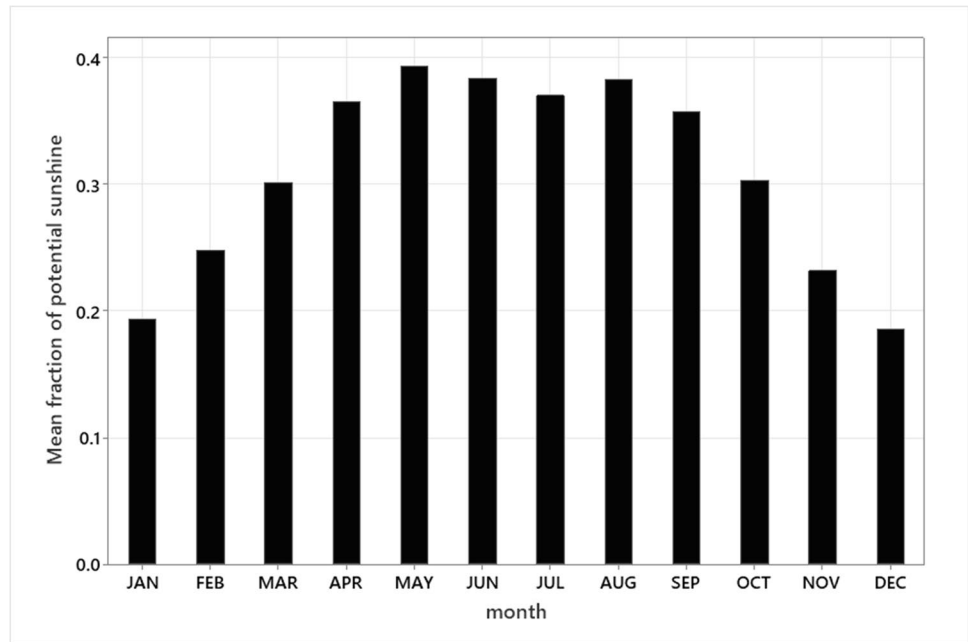
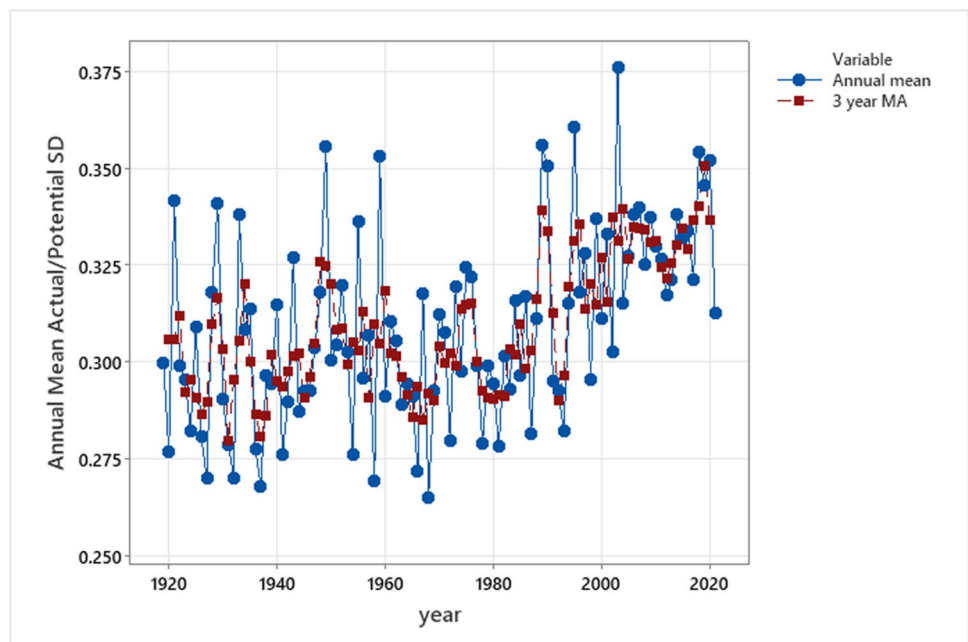


Fig. 10 Mean annual sunshine fraction (observed SD hours/maximum potential SD hours) and a 3-year moving average for England series 1919–2021



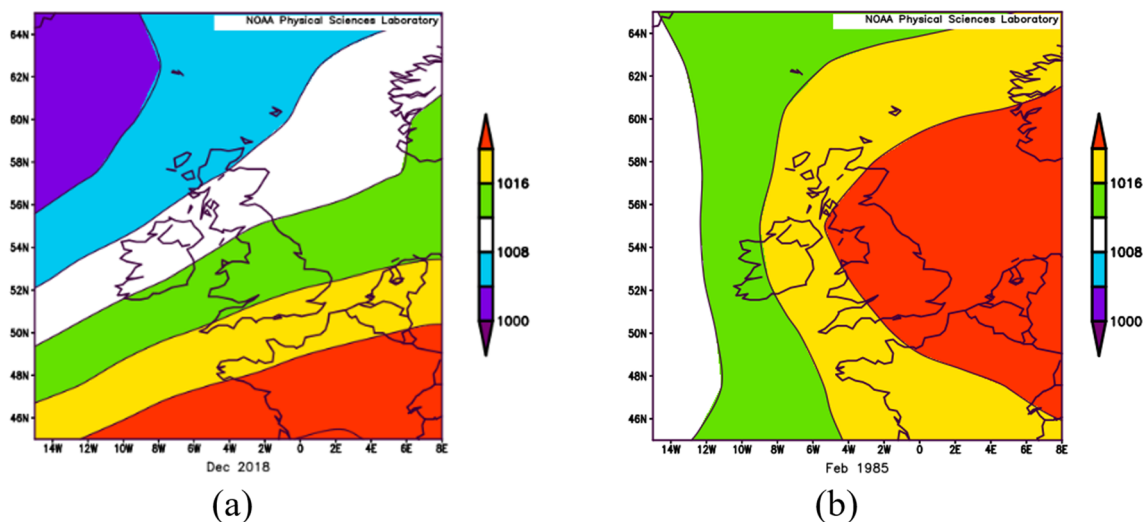
variability in the dataset, and annual SD has begun to level off, but what is particularly noticeable is the decrease in occurrences of years with low levels of sunshine. Since 2000, there has been no year which has recorded annual total amounts less than the median of the full record. This continuation of the brightening observed by other authors is evident in subregions of England, with the linear trend in increasing sunshine hours strongest in the Northeast at a rate of 51 h, a decade since 1985. The increase in total sunshine in all regions is significant in all seasons except for summer and is strongest in the winter months. In the

Midlands region, in the two decades between 2000 and 2019, winter totals averaged 190 h, some 36% more than period 1920–1939. Progressive improvements in air quality and a reduction in fog formation could be associated with this increased sunshine. In 1970, UK sulphur dioxide emissions were at an all-time maximum in the region of 6.5 Mt of sulphur dioxide (DEFRA 2022), and the steep decline in this gas (a proxy for emissions of black carbon in smoke) is presumably related to increasing sunshine. There is a strong statistical correlation, but this need not indicate a wholly causative relationship.

Table 3 Mean and standard deviations of UK synoptic indices

	Mean <i>P</i> (SD)	Mean <i>W</i> (SD)	Mean <i>S</i> (SD)	Mean <i>F</i> (SD)	Mean <i>Z</i> (SD)
Winter	1010.78 (5.60)	9.36 (7.53)	4.47 (5.74)	19.91 (4.09)	0.56 (12.56)
Spring	1013.69 (3.57)	3.84 (5.67)	2.14 (4.09)	14.56 (3.40)	-0.89 (10.43)
Summer	1014.38 (2.23)	5.22 (3.11)	0.83 (2.57)	11.32 (1.84)	-0.59 (8.37)
Autumn	1011.75 (3.91)	7.52 (5.00)	3.04 (4.56)	16.52 (3.21)	0.46 (11.26)
F	53.82*	59.72*	37.68*	380.63*	1.44

*Significant difference at 0.05

**Fig. 11** **a** Monthly mean sea-level pressure (hPa) December 2018 and **b** February 1985

4.2 Synoptic indices for the British Isles

Application of the JC technique for an equivalent time period as the SD data produces a catalogue of 27 weather types with some principal types (notably A, C, W, SW, NW and S). Table 3 lists characteristics of the atmospheric circulation indices (upon which weather types are based), and considerable seasonal variability is evident. Applications of ANOVA and post hoc Fisher's test indicate that *P*, *W*, *S* and *F* values are significantly different at 0.05 level between all seasons. Mean circulation displays a distinctly stronger south westerly flow in winter than at other times of the year. *Z* is the only synoptic index that displays no significant coherent between-season variability, although there are considerable within-season differences from year-to-year. Figure 11a shows a monthly sea level pattern (December 2018) that approximates to winter normals for all circulation indices and a winter month (Fig. 11b), February 1985, with high values for the meridional ($S = +12.15$) and vorticity ($Z = -19.29$) indices. Over the time period examined (1919–2021), there has been a small but significant increase in the zonal *W* index (not present in summer) and an accompanying reduction in meridionality (*S* index); however, no annual or season-based trend in other indices can be identified.

4.3 Synoptic analysis of SD series in England and regions

The influence of daily weather types can be assessed using solar radiation data, as daily sunshine duration data on MIDAS is incomplete. SW England insolation measurements recorded at Camborne in the SW England region² also indicate a clear control by the main weather types.³ Figure 12 shows that, in summer, radiation recorded on anticyclonic days contrasts strongly with cyclonic and westerly days ($p < 0.001$).

Monthly index values can be used to identify synoptic controls on sunshine fraction. Stepwise regression using synoptic indices as predictor variables was applied to mean monthly sunshine fraction, and results are presented in Table 4. The all-season synoptic control on the England series is strong ($R^2 = 42.0\%$) but is more important when sunshine duration and radiation intensity are greatest in summer and spring. There is still a limited control in winter ($R^2 = 11.5\%$), but the cloud effect on radiation is dampened

² Identified later as the region's most associated with synoptic controls.

³ Using Lamb (1972) original seven types plus U.

Fig. 12 Summer mean solar irradiance for principal weather types in Camborne ($F=124.66$, $p<0.001$)

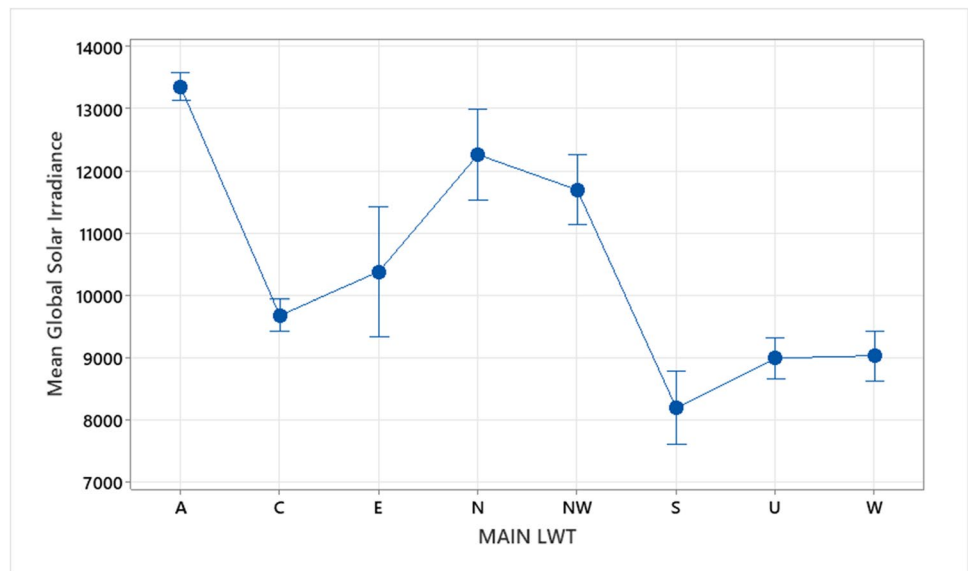


Table 4 Results of stepwise regression between observed sunshine fraction and synoptic index predictors (significant at 0.05) 1919–2021

	Stepwise regression model (based on the England sunshine series)	Stepwise regression model (Regression models with the best performing regional sunshine series—highest R^2 are listed)
All months	$0.4848 - 0.00953F - 0.00322Z$; $R^2 = 42.0\%$, $F = 46.76$; $p < 0.001$	$0.5501 + 0.00413W - 0.0167F - 0.00190Z$; $R^2 = 45.7\%$, $F = 359.07$; $p < 0.001$ (southwest)
Spring	$0.4386 + 0.00456P + 0.00696W + 0.00269S - 0.01247F - 0.001163F$; $R^2 = 34.7\%$, $F = 32.23$; $p < 0.001$	$0.5063 + 0.0030P + 0.00557W - 0.01388F - 0.00215Z$; $R^2 = 44.7\%$, $F = 61.51$; $p < 0.001$ (southwest)
Summer	$0.3940 - 0.00411W + 0.00747S - 0.00408F - 0.00536Z$; $R^2 = 45.4\%$, $F = 63.16$; $p < 0.001$	$0.3819 + 0.06646Z$ $R^2 = 46.7\%$, $F = 268.98$; $p < 0.001$ (southwest)
Autumn	$0.4388 + 0.00588W - 0.01122F - 0.00099Z$; $R^2 = 21.8\%$, $F = 28.42$; $p < 0.001$	$0.4823 + 0.00339W - 0.01252F - 0.00122Z$; $R^2 = 28.4\%$, $F = 40.26$; $p < 0.001$ (southwest)
Winter	$0.2035 - 0.00162W - 0.00217S$; $R^2 = 11.5\%$, $F = 13.11$; $p < 0.001$	$0.2313 - 0.00282P + 0.00231W - 0.00355S$; $R^2 = 22.2\%$, $F = 21.73$; $p < 0.001$ (northeast)

by the weaker sun. Vorticity is the dominant control on sunshine fraction (negative vorticity suppressing the ascent of air and reducing cloud cover); yet, westerly flow also increases observed sunshine despite the Atlantic origin of air masses. During the year, vorticity and southerly meridional flow exert an influence. Subregions display a similar circulation-response to the England series particularly in the Southwest, followed by the Northwest region. These areas are much more likely to develop cloudy skies under relatively frequent humid southwest and westerly flows than other downwind regions where cloud development is variable.

Examples of synoptic controls on SD in summer are given in Fig. 13. June 2012 exhibited well below average sunshine (England 117.9 h, 64% of June mean) due to the strong cyclonicity. There were 15 ‘C’ days compared to the mean of 4, and the Z index was 16.89 ($z = 2.1^4$). The strongly anti-cyclonic (22 ‘A’ type days; $Z = -20.17$ ($z = -2.3^5$)) month of August 1976 received 136% of the August mean SD.

4.4 Changes to daily weather type—solar radiation association

Despite this pronounced synoptic control, the positive trend in sunshine since the mid-1980s cannot be directly explained by any trend in circulation in the British Isles region during this period. For instance, in recent decades, there has been a slight, but significant, decrease in zonal westerlies and an increase in vorticity. Given the relationships established in Table 4, both of these cannot be explanatory of the brightening. Given that there is no change detected in the occurrence of influential synoptic controls, it can be assumed that the brightening is independent of circulation. Daily solar

⁴ A z score of 2.1 represents a probability of 1.786% of a month occurring with this fraction of sunshine.

⁵ A z score of -2.3 represents a probability of 1.072% of a month occurring with this fraction of sunshine.

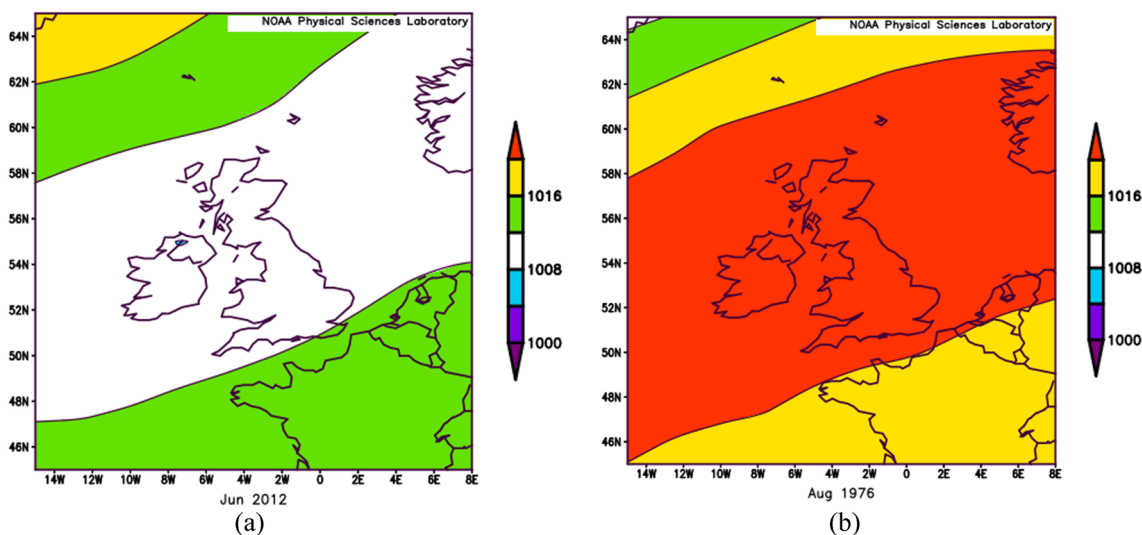
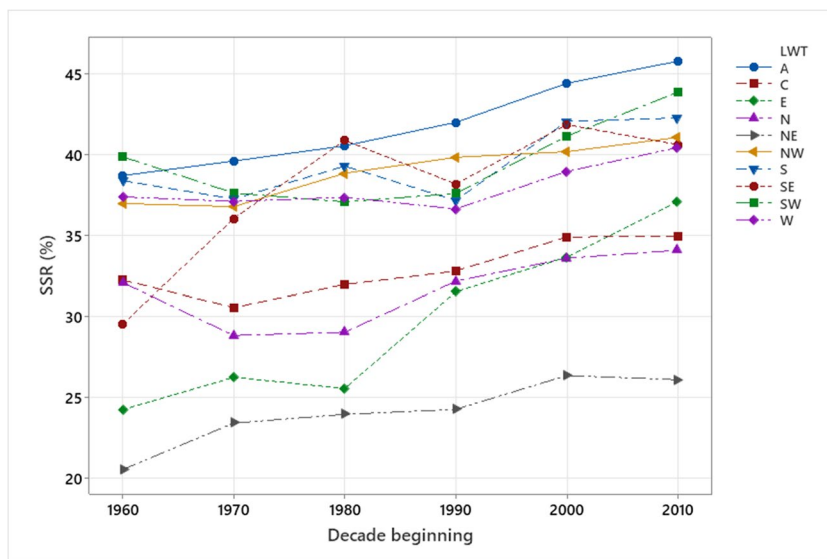


Fig. 13 **a** Sea-level pressure (hPa) charts related to low levels of sunshine (64% of summer England mean) due to high cyclonicity in June 2012 ($Z = +16.89$) compared to **b** high level of sunshine in August

1976 (136% of normal hours) ($Z = -20.17$ ($z = -2.3$)). (A z score of -2.3 represents a probability of 1.072% of a month occurring with this fraction of sunshine.)

Fig. 14 shows decadal means of daily solar radiation fraction data under selected weather types from East Malling, SE England



radiation receipt under each daily weather type was then investigated to determine if the association was stationary (constant) in the time period.

Interestingly, all of the main types display an increase in mean radiation, but this is greater under some weather types (Fig. 14). For example, although the decadal mean of the fraction of maximum solar radiation in 2010–2019 increased by almost 8% from the decadal mean in 1960–1969, for easterly type days, this increase has been considerably greater at 13%. This latter increase might reflect the contribution of improvements in air quality as easterly weather types have been shown elsewhere (Graham et al. 2020) to be associated with transported

particulate matter from Northwest Europe. Along with SE types, E types display the greatest increases in radiation when the type occurs. Cleaner air masses from the Atlantic, such as W and SW have had less significant radiation increases.

5 Concluding remarks

This study examines the sunshine duration data series in England and subregions. It is clear that the brightening trend first observed by authors almost two decades ago has continued. Mean decadal sunshine fraction in the England series

2010–2019 was 2.5% higher than in 1920–1929 representing an increase in annual mean duration of over 106 h. This has been observed at a time when traditional instruments for the measurement of SD (Campbell-Stokes recorders) are being progressively replaced by automatic sensors, and some investigators (*e.g.* Matuszko 2015) have even suggested that SD data should be treated with caution, especially as automatic sensors may be more sensitive and record higher SD hours. It is interesting to note in Fig. 2 that there are no years in Bradford with observed sunshine total of less than 1240 h after 2000. At this station, there has been concurrent use of C-S recorders and automatic sensors, and since 2000, over 53% of the monthly SD totals plotted in Fig. 2 are from the pyranometer. This suggests possible inhomogeneity in the series; however, the plot of adjusted sunshine series areal data also shows few below long-term mean values after 2000, and this suggests that this is a real change rather than a measurement issue. Furthermore, the increases in sunshine recorded at ground-based stations matches that found in the solar irradiance measurements at representative UK locations and estimates using satellite imagery (*e.g.* Copernicus 2022).

Explanations for the brightening trend continue to warrant further research. It is commonly accepted that the reduction in emissions of black smoke and other pollutants will have contributed to the brightening by reducing the opacity of the atmosphere to short wave radiation. The effect of a reduction in transboundary pollution from Europe is evident by the considerable increase in radiation measured at East Malling, Kent, under easterly days. Furthermore, in the UK, straw and stubble burning was widespread in the 1970s and early 1980s and may well have had an impact on late summer and autumn sunshine amounts. On the other hand, the effect of anthropogenic sources could have been over-estimated as improvements in the quality of the atmosphere began to level off after 2000, yet SD continues to rise.

Atmospheric circulation changes, which are strongly related to cloud coverage, are considered as key to any explanation. This study uses the surface-based method developed by Jenkinson and Collison for the British Isles. It identifies a strong synoptic control with a increased sunshine fraction being strongly related to negative vorticity (anticyclonicity) and, to some extent, westerly flow and other indices. One of the main limitations of pressure pattern classification relates to the lack of information about weather fronts. Mid-latitude circulation on any one day often features an extensive system of fronts, as opposed to the ‘front-free’ atmosphere of low latitudes. Physical properties of polar and tropical air masses can differ so greatly that they are sharply separated by frontal surfaces. Cloud systems form in frontal convergence zones and are commonly much more extensive horizontally and vertically than individual cloud systems building up due to thermal convection in a uniform air mass. Fronts, therefore, have

a considerable impact indirectly on surface solar radiation receipt and sunshine duration.

As no significant trend in either the frequency of weather types or trends in synoptic indices can be detected, it does indicate that circulation patterns alone have not accounted for the change in radiation. It is suggested that the relationship between circulation and SD is not stationary across the time period and that, in addition to the general reduction in aerosols, there is another mechanism in operation that this surface level synoptic method fails to capture. This is likely to be related to cloud formation which occurs at different levels in the atmosphere and is unrelated to surface flow alone. Summer thunderstorms with anticyclonic weather types, for example, are most likely to be associated with upper troughs circulating the high pressure centre. This includes changes in cloud type, height, depth or even physical properties. It is pertinent, therefore, to consider circulation patterns at higher levels in the atmosphere and associated cloud processes.

Understanding the nature of the solar resource is critical at this point in time to develop further a zero carbon, cheaper domestic energy source. Despite the relatively low levels of potential solar radiation in the UK, considerably more power could be harnessed from this clean source, and it is a positive that, whatever the reason, the quantity of this resource is increasing.

Author contribution GS and DB conceived the study, collected the data, conducted the research, wrote the manuscript and prepared the figures within. Both authors read and approved the final manuscript.

Data availability Data used in this study are freely available from the UK Met Office climate series page at <https://www.metoffice.gov.uk/research/climate/maps-and-data/about/archives>. The datasets used and analysed in this study are available from the UK Met Office here <https://www.metoffice.gov.uk/research/climate/maps-and-data/uk-and-regional-series>

Code availability Not applicable.

Declarations

Ethics approval The authors declare that due to the nature of the research, there was no requirement for any ethics approval to be sought.

Consent to participate Not applicable.

Consent for publication Not applicable.

Competing interests The authors declare no competing interests.

Open Access This article is licensed under a Creative Commons Attribution 4.0 International License, which permits use, sharing, adaptation, distribution and reproduction in any medium or format, as long as you give appropriate credit to the original author(s) and the source, provide a link to the Creative Commons licence, and indicate if changes were made. The images or other third party material in this article are

included in the article's Creative Commons licence, unless indicated otherwise in a credit line to the material. If material is not included in the article's Creative Commons licence and your intended use is not permitted by statutory regulation or exceeds the permitted use, you will need to obtain permission directly from the copyright holder. To view a copy of this licence, visit <http://creativecommons.org/licenses/by/4.0/>.

References

- Alpert P, Kishcha Y, Kaufman J, Schwarzbard R (2005) Global dimming or local dimming?: Effect of urbanization on sunlight availability. *Geophys Res Lett* 32:L17802. <https://doi.org/10.1029/2005GL023320>
- Arnell NW, Freeman A (2021) The effect of climate change on agroclimatic indicators in the UK. *Climatic Change* 165:40. <https://doi.org/10.1007/s10584-021-03054-8>
- Augustine JA, Dutton EG (2013) Variability of the surface radiation budget over the United States from 1996 through 2011 from high-quality measurements. *J Geophys Res Atmos* 118:43–53. <https://doi.org/10.1029/2012JD018551>
- BP (2022) *Statistical Review of World Energy* <https://www.bp.com/en/global/corporate/energy-economics/statistical-review-of-world-energy.html> (accessed 01.08.22)
- Brisson E, Demuzere M, Kwakernaak B, Van Lipzig NPM (2011) Relations between atmospheric circulation and precipitation in Belgium. *Meteorol Atmos Phys* 11:27–39. <https://doi.org/10.1007/s00703-010-0103-y>
- Buishand TA, Brandsma T (1997) Comparison of circulation classification schemes for predicting temperature and precipitation in the Netherlands. *Int J Climatol* 17:875–889. [https://doi.org/10.1002/\(SICI\)1097-0088\(19970630\)17:8%3c875::AIDJOC164%3e3.0.CO;2-C](https://doi.org/10.1002/(SICI)1097-0088(19970630)17:8%3c875::AIDJOC164%3e3.0.CO;2-C)
- Burnett D, Barbour E, Harrison GP (2014) The UK solar energy resource and the impact of climate change. *Renewable Energy* 71:333–343. <https://doi.org/10.1016/j.renene.2014.05.034>
- Chen D (2000) A monthly circulation climatology for Sweden and its application to a winter temperature case study. *Int J Climatol* 20:1067–1076. [https://doi.org/10.1002/1097-0088\(200008\)20:103.0.CO;2-Q](https://doi.org/10.1002/1097-0088(200008)20:103.0.CO;2-Q)
- Copernicus (2022) *European State of the Climate. Clouds and sunshine duration*. <https://climate.copernicus.eu/esotc/2021/clouds-and-sunshine-duration> (Accessed 01.08.22)
- CRU (2022) <https://crudata.uea.ac.uk/cru/data/lwt/> (Accessed 01.08.22)
- Cutforth H, Judiesch D (2007) Long-term changes to incoming solar energy on the Canadian Prairie. *Agric for Meteorol* 145:167–175. <https://doi.org/10.1016/j.agrformet.2007.04.011>
- DEFRA (2022) *National statistics, emissions of air pollutants in the UK – sulphur dioxide (SO₂)*. (Accessed 01.08.22)
- GEBA (2022) <https://geba.ethz.ch/> (Accessed 01.08.22)
- Graham AM, Pringle KJ, Arnold SR, Pope RJ, Vieno M, Butt EW, Conibear L, Stirling EL, McQuaid JB (2020) Impact of weather types on UK ambient particulate matter concentrations. *Atmospheric Environment: X* 5:100061. <https://doi.org/10.1016/j.aeaoa.2019.100061>
- Grise KM, Polvani LM (2014) Southern hemisphere cloud-dynamics biases in CMIP5 models and their implications for climate projections. *J Clim* 27:6074–6092. <https://doi.org/10.1175/JCLI-D-14-00113.1>
- Hollis D, McCarthy MP, Kendon M, Legg T, Simpson I (2019) HadUK-Grid—A new UK dataset of gridded climate observations. *Geosci Data J* 6:151–159. <https://doi.org/10.1002/gdj3.78>
- IPCC (2007) *Climate Change 2007: the physical science basis. Contribution of working group I to the fourth assessment report of the Intergovernmental Panel on Climate Change* [Solomon SD Qin M Manning Z Chen M Marquis KB Avery T Tignor M Miller HL (eds.)] Cambridge University Press, Cambridge, United Kingdom and New York, NY, USA
- Jenkinson AF, Collinson FP (1977) An initial climatology of gales over the North Sea. *Synoptic Climatol Branch Memorandum* 62:18
- Kalnay E, Kanamitsu M, Kistler R, Collins W, Deaven D, Gandin L, Iredel M, Saha S, White G, Wollen J, Zhu Y, Chelliah M, Ebisuzaki W, Higgins W, Janowiak J, Mo KC, Ropelewski C, Wang J, Leetmaa A, Reynolds R, Jenne R, Joseph D (1996) The NCEP/NCAR 40-year reanalysis project. *Bull Am Meteor Soc* 77:437–471. [https://doi.org/10.1175/1520-0477\(1996\)077%3c0437:TNYRP%3e2.0.CO;2](https://doi.org/10.1175/1520-0477(1996)077%3c0437:TNYRP%3e2.0.CO;2)
- Kerr A, Tabony R (2004) Comparison of sunshine recorded by Campbell-Stokes and automatic sensors. *Weather* 59:90–95. <https://doi.org/10.1256/wea.99.03>
- Lamb HH (1972) *British Isles Weather types and a register of daily sequence of circulation patterns, 1861–1971*. Geophysical Memoir 116 HMSO, London
- Legg T (2014) Comparison of daily sunshine duration recorded by Campbell-Stokes and Kipp and Zonen sensors. *Weather* 69:264–269. <https://doi.org/10.1002/wea.2288>
- Liepert BG (2002) Observed reductions of surface solar radiation at sites in the United States and worldwide from 1961 to 1990. *Geophys. Res Lett* 29:1421. <https://doi.org/10.1029/2002GL014910>
- Linderson M-L (2001) Objective classification of atmospheric circulation over southern Scandinavia. *Int J Climatol* 21:155–169. <https://doi.org/10.1002/joc.604>
- Matuszko D (2012) Influence of cloudiness on sunshine duration. *Int J Climatol* 32:1527–1536. <https://doi.org/10.1002/joc.2370>
- Matuszko D (2015) A comparison of sunshine duration records from the Campbell-Stokes sunshine recorder and CSD3 sunshine duration sensor. *Theor Appl Climatol* 119:401–406. <https://doi.org/10.1007/s00704-014-1125-z>
- Met Office (2019) Met Office MIDAS Open: UK land surface stations data (1853-current). Centre for Environmental Data Analysis. (Accessed 01.07.22)
- Miró Cubells JR, Pepin N, Peña JC, Martín-Vide J (2020) Daily atmospheric circulation patterns for Catalonia (northeast Iberian Peninsula) using a modified version of Jenkinson and Collinson method. *Atmos Res* 231:104674. <https://doi.org/10.1016/j.atmosres.2019.104674>
- Osipova IP, Osipov EY (2022) Objective classification of weather types for the Eastern Siberia over the 1970–2020 period using the Jenkinson and Collinson method. *Atmos Res* 277:106291. <https://doi.org/10.1016/j.atmosres.2022.106291>
- Painter HE (1981) The performance of a Campbell-Stokes sunshine recorder compared with a simultaneous record of the normal incidence irradiance. *Meteorol Mag* 110:102–109
- Papavasileiou G, Voigt A, Knippertz P (2020) The role of observed cloud-radiative anomalies for the dynamics of the North Atlantic oscillation on synoptic time-scales. *Q J R Meteorol Soc* 146:1822–1841. <https://doi.org/10.1002/qj.3768>
- Perry M (2007) Updated comparison of sunshine duration recorded by Campbell-Stokes and automatic sensors. NCIC Memorandum no. 27 (2011). National Meteorological Library: Exeter, UK
- Pope RJ, Savage NH, Chipperfield MP, Arnold SR, Osborn TJ (2014) The influence of synoptic weather regimes on UK air quality: analysis of satellite column NO₂. *Atmos Sci Lett* 15:211–217. <https://doi.org/10.1002/asl2.492>
- Pozo-Vázquez D, Tovar-Pescador J, Gámiz-Fortis SR, Esteban-Parra M, Castro-Díez Y (2004) NAO and solar radiation variability in the

- European North Atlantic region. *Geophys Res Lett* 31(5):L05201. <https://doi.org/10.1029/2003gl018502>
- Prescott J (1940) Evaporation from water surface in relation to solar radiation. *Trans Royal Soc Aust* 64:114–118
- Psistaki K, Paschalidou AK, McGregor G (2020) Weather patterns and all-cause mortality in England, UK. *Int J Biometeorol* 64:123–136. <https://doi.org/10.1007/s00484-019-01803-0>
- Putnikovic S, Tomic I, Đurđević V (2016) Circulation weather types and their influence on precipitation in Serbia. *Meteorol Atmos Phys* 128:649–662. <https://doi.org/10.1007/s00703-016-0432-6>
- Ritchie H, Roser M (2022) Renewable Energy. <https://ourworldindata.org/renewable-energy> (Accessed 01.07.22)
- Sanchez-Lorenzo A, Calbo J, Martín-Vide J (2008) Spatial and temporal trends in sunshine duration over western Europe (1938–2004). *J Clim* 21:6089–6098. <https://doi.org/10.1175/2008JCLI2442.1>
- Sanchez-Romero A, Sanchez-Lorenzo A, Calbó González JA, Azorín-Molina C (2014) The signal of aerosol-induced changes in sunshine duration records: a review of the evidence. *J Geophys Res: Atmospheres* 119:4657–4673. <https://doi.org/10.1002/2013JD021393>
- Sarricolea P, Meseguer-Ruiz O, Martín-Vide J, Outeiro L (2018) Trends in the frequency of synoptic types in Central-Southern Chile in the period 1961–2012 using the Jenkinson and Collinson synoptic classification. *Theor Appl Climatol* 134:193–204. <https://doi.org/10.1007/s00704-017-2268-5>
- Spellman G (2017) An assessment of the Jenkinson and Collinson synoptic classification to a continental mid-latitude location. *Theor Appl Climatol* 128:731–744. <https://doi.org/10.1007/s00704-015-1711-8>
- Srinivasa R, Macara G, Liley B (2019) Sunshine duration instrument comparisons in New Zealand. *Weather and Climate* 39:28–41. <https://doi.org/10.2307/26892910>
- Stanhill GH, Cohen S (2001) Global dimming: a review of the evidence for a widespread and significant reduction in global radiation with a discussion of its probable causes and possible agricultural consequences. *Agric for Meteorol* 107:255–278. [https://doi.org/10.1016/S0168-1923\(00\)00241-0](https://doi.org/10.1016/S0168-1923(00)00241-0)
- Stanhill G, Achima O, Rosa Cohen S (2014) The cause of solar dimming and brightening at the Earth's surface during the last half century: evidence from measurements of sunshine duration. *J Geophys Res Atmos* 119:10902–10911. <https://doi.org/10.1002/2013JD021308>
- Streets DG, Chin Yan M, Diehl T, Mahowald N, Schultz M, Wild M, Wu YM, Yu C (2009) Anthropogenic and natural contributions to regional trends in aerosol optical depth, 1980–2006. *J Geophys Res* 114:D00D18. <https://doi.org/10.1029/2008JD011624>
- Suehrck H (2000) On the relationship between duration of sunshine and solar radiation on the earth's surface. *Solar Energy* 68:417–42. [https://doi.org/10.1016/S0038-092X\(00\)00004-9](https://doi.org/10.1016/S0038-092X(00)00004-9)
- Taniguchi K, Takano M, Tobar Y, Hayano M, Nakajima S, Mimura M, Tsubota K, Noda Y (2022) Influence of external natural environment including sunshine exposure on public mental health: a systematic review. *Psychiatry Int* 3:91–113. <https://doi.org/10.3390/psychiatryint3010008>
- Taylor T, Ortiz R (2001) Impacts of climate change on domestic tourism in the UK: a panel data estimation. *Tour Econ* 15:803–812. <https://doi.org/10.5367/000000009789955>
- Urban G, Zajac I (2017) Comparison of sunshine duration measurements from Campbell-Stokes sunshine recorder and CSD1 sensor. *Theor Appl Climatol* 129:77–87
- Urban G, Mięgała K, Pawliczek P (2018) Sunshine duration and its variability in the main ridge of the Karkonosze Mountains in relation to with atmospheric circulation. *Theor Appl Climatol* 131:1173. <https://doi.org/10.1007/s00704-017-2035-7>
- Van Heerwaarden CC, Mol WB, Veerman MA, Benedict I, Heu-sinkveld BG, Knap WH, Kazadzis S, Kouremeti N, Fiedler S (2021) Record high solar irradiance in Western Europe during first COVID-19 lockdown largely due to unusual weather. *Commun Earth Environ* 2:37. <https://doi.org/10.1038/s43247-021-00110-0>
- Voigt A, Alber N, Ceppi P, Grise K, Li Y, Medeiro B (2020) Clouds, radiation, and atmospheric circulation in the present-day climate and under climate change. *WIREs Clim Change* 12, pp 22. <https://doi.org/10.1002/wcc.694>
- Wang K, Dickinson EE, Wild M, Liang S (2012) Atmospheric impacts on climatic variability of surface incident solar radiation. *Atmos Chem Phys* 12:14009–14042. <https://doi.org/10.5194/acp-12-9581-2012>
- Wild M (2009) Global dimming and brightening: a review. *J Geophys Res* 114:D10. <https://doi.org/10.1029/2008JD011470>
- Wild M, Gilgen H, Roesch A, Ohmura A, Long C, Dutton E, Forgan B, Kallis A, Russak V, Tsvetkov A (2005) From dimming to brightening: decadal changes in solar radiation at the Earth's surface. *Science* 308:847–850. <https://doi.org/10.1126/science.1103215>
- World Meteorological Organization (2008) Guide to meteorological instruments and methods of observation: (CIMO guide). WMO No.8 Secretariat of the WMO Geneva Switzerland

Publisher's Note Springer Nature remains neutral with regard to jurisdictional claims in published maps and institutional affiliations.